Biosensors and Bioelectronics 157 (2020) 112151

Contents lists available at ScienceDirect

Biosensors and Bioelectronics

journal homepage: http://www.elsevier.com/locate/bios

An optical-based biosensor of the epithelial sodium channel as a tool for diagnosing hypertension

Diana L. García-Rubio [a,**], M.B. de la Mora [b,*], Doris Cerecedo [a], José M. Saniger Blesa [c], M. Villagrán-Muniz [c]

[a] Laboratorio de Hematobiología, Escuela Nacional de Medicina y Homeopatía, Instituto Politécnico Nacional, Mexico City, Mexico
[b] CONACyT Fellow-ICAT, Universidad Nacional Autónoma de México, Mexico City, Mexico
[c] Instituto de Ciencias Aplicadas y Tecnología, Universidad Nacional Autónoma de México, Mexico City, Mexico

ARTICLE INFO

Keywords:
Biosensor
Hypertension
Functionalization
Gold nanoparticles
Epithelial sodium channel

ABSTRACT

Arterial hypertension (HTN) is a world health concern presenting difficulties for its early detection. It leads to cardiovascular and kidney complications that increase morbidity in adults. Overexpression in the epithelial sodium channel (ENaC) in membrane platelets can be related with the presence of HTN and thus can be used as a biomarker to detect this medical condition. Here, we propose a method for HTN diagnosis based on gold nanoparticles (GNPs) conjugated to an antibody against the ENaC present on platelets. These functionalized GNPs were analyzed by Zeta potential, dynamic light scattering, electron microscopy, and other spectroscopic techniques. To verify that the GNPs and α-ENaC antibodies formed conjugates (GNPs-antiENaC) that maintained their specificity to the target, we carried out an indirect immunofluorescence detection assay of GNPs-antiENaC bound to a secondary antibody labeled with a fluorophore. Our results show that the presence of GNPs increase the fluorescence intensity in platelets treated with GNPs-antiENaC conjugates. It is also observed a clear tendency of the fluorescence signal in platelets treated with the conjugates that could be used for discrimination between normotensive and hypertensive samples. The proposed assay can be implemented as a very sensitive routine test to diagnose HTN.

1. Introduction

Arterial hypertension (HTN) is a clinical condition defined as a persistent high blood pressure. Values of systolic and diastolic pressure equal to or greater than 140 and 90 mmHg, respectively, are considered as indicators that a person experiences hypertension. According to the World Health Organization, 1.13 billion people worldwide have hypertension (Organization, 2019). However, approximately 40% of adults suffer from hypertension and are not appropriately diagnosed in a timely manner. This fact strongly suggests that the established protocols to diagnose HTN are not effective. While HTN lacks symptoms and the standard blood pressure measurement is very susceptible to variations due to situations not related to the disease, its detection and timely diagnosis is even more difficult. Blood pressure is controlled by the kidney trough modulating the total body sodium content through the epithelial sodium channel (ENaC), and its deregulation is directly associated with HTN. 50% of hypertensive individuals are sensitive to sodium, which is regulated in the distal nephron through the ENaC (Hanukoglu and Hanukoglu, 2016). Deregulation of this ion channel is directly associated with HTN (Bhalla and Hallows, 2008), since it also participates in the retention of sodium in the epithelial cells of the distal colon, the duct of several endocrine glands and the lung (Enuka et al., 2012).

The presence of a constant high blood pressure exhibits a strong correlation with risk of stroke and heart failure and/or kidney disease. Moreover, several studies have shown that a constant high-pressure lead to a pre-activation state that affects the biochemical composition and by consequence the performance of blood cells. For example, changes in the lipidic compositions of erythrocytes made them prone to lysis (Martínez-Vieyra et al., 2019), neutrophils circulate while activated, generating high quantities of reactive oxygen species (Reus-Chavarría et al., 2019), while modification in the protein and lipid contents in platelets trigger their activation (Cerecedo et al., 2016). Among the modifications found in platelets, it was the overexpression of the epithelial sodium

* Corresponding author.
** Corresponding author.
E-mail addresses: diana_23_x@hotmail.com (D.L. García-Rubio), maria.delamora@gmail.com (M.B. de la Mora).

https://doi.org/10.1016/j.bios.2020.112151
Received 26 October 2019; Received in revised form 4 March 2020; Accepted 11 March 2020
Available online 14 March 2020

channel (ENaC) that we have proposed and validated by biochemical techniques (Western-blot) and molecular biology as quantitative reverse transcription polymerase chain reaction (qRT-PCR) techniques for use as a biomarker to diagnose HTN.

The quantification of biomarkers can be made by different approaches such as electrochemical or chemical response, immunochemistry and optical methods, along with others (Mascini and Tombelli, 2008). In particular, optical techniques are based on the association of a molecule of interest with a material or molecule that exhibit a typical optical response such as transmittance, reflectance, fluorescence, Raman response, among others (Borisov and Wolfbeis, 2008). Once the molecule of interest is attached to the material, the typical optical response presents a shift proportional to the amount of the analyte. Recently, metal nanoparticles have been successfully used as optical biosensors due to their exceptional optical properties as the presence of surface plasmon resonance (SPR) (Doria et al., 2012; Lazarides et al., 2000). As a consequence of the SPR, metal nanoparticles present a strong absorption band that is very sensitive to changes in the surroundings of the surface of the nanoparticles. Also, the SPR can interact with the near electric field of molecules and materials, generating an intensification of optical signals such as fluorescence (Kang et al., 2011) or Raman responses (Qian and Nie, 2008). Due to their chemical, surface, and plasmonic (SPR) response, gold nanoparticles (GNPs) are one of the most extensively used metal nanoparticles for biosensing (Devi et al., 2015; Larguinho and Baptista, 2012).

The use of gold nanoparticles to increase the sensitivity of a fluorophore has been explored by several research groups (Acuna et al., 2012; Kang et al., 2011; Nakamura and Hayashi, 2005). While there are successful implementations, there are also examples where the fluorescent signal is quenched (Schneider et al., 2006). The dynamic of the interaction is complex and depends on several factors—for example, the absorption and emission wavelengths of the fluorophore, the plasmonic response of the gold nanoparticle and the distance from the nanoparticle to the fluorophore. When the distance is optimal, the optical signal of a fluorophore that is close to the nanoparticles is enhanced, facilitating its measurement (Iosin et al., 2009).

Since the techniques employed to quantify the ENaC involve expensive inputs and qualified personnel for their realization, in this work we propose the coupling of ENaC antibody to GNPs followed by fluorescent labeling of these conjugates and their interaction with platelets as a strategy to quantitatively detect and characterize the differential presence of ENaC in platelets of both normotensive and hypertensive individuals.

A common method utilized for the preparation of biocompatible gold nanoparticles is based on bi-functional molecules containing both a thiol and a carboxylic group. While the thiol group binds to the gold surface, the carboxylic group is the binding site to conjugate protein molecules such as antibodies and peptides through amide bonds (Bartczak and Kanaras, 2011). A popular strategy to achieve this chemical conjugation is the use of N-(3-dimethylaminopropyl)-N′-ethylcarbodiimide hydrochloride (EDC) and hydroxy-2,5-dioxopyrrolidine-3-sulfonicacid (Sulfo NHS), together known as NHS-EDC chemistry (Quarta et al., 2012). Here, we propose to use this methodology to bind colloidal gold nanoparticles to the ENaC present in platelets. Then, we perform a careful characterization of the functionalized colloidal nanoparticles as well as the interaction among the colloidal system with platelets of normotensive (NT) and hypertensive individuals. Finally, the ability of these gold nanoparticles to detect HTN was tested using an immunofluorescence assay.

2. Materials and methods

2.1. Materials

Gold nanoparticles of about 30 nm in diameter, stabilized in a suspension of 0.1 mM Phosphate-buffered saline (PBS), 3-mercaptopropionic acid (MPA), Buffer 2-(N-morpholino) ethanesulfonic acid (MES), were all purchased from Sigma Aldrich. Sodium-channel alpha-rabbit polyclonal antibody (cat. no. PA5-35364) was obtained from Invitrogen, Carlsbad, CA, USA, and bovine serum albumin (BSA) and fluorescent dye Alexa fluor 488 were purchased from Molecular Probes (Eugene, OR, USA). Bi-distilled water and phosphate buffered saline (PBS) were used for washing and rinsing of samples before and after conjugation procedures, respectively.

2.2. Obtention of human platelets

Blood samples were obtained from normotensive (NH) and hypertensive (HTN) individuals and mixed with a citrate anticoagulant at pH 6.5 (19:16 NT: HTN; see details of the study population in Appendix A; Table A.1). Platelet-rich plasma was obtained from the total blood by centrifugation at 100×*g* for 20 min at room temperature. Plasma was subsequently mixed with an equal volume of citrate anticoagulant and centrifuged at 400×*g* for 10 min. The platelet pack was suspended and washed twice with Hank's Balanced Saline Solution without calcium and finally suspended in PBS.

2.3. Obtention and characterization GNPs-anti-ENaC conjugates

2.3.1. Functionalization of GNPs with MPA

Gold nanoparticles (Sigma-Aldrich Cat. Num. 753629) were used at an approximate concentration of 4.5×10^{10} particles/mL, 80 μM of 3-mercaptopropionic acid (MPA) in a water solution was added in approximately a 1:1 vol ratio. The mixture was then sonicated for about 1 h to ensure complete functionalization of the nanoparticles.

2.3.2. Carboxylic group activation and GNPs-anti-ENaC conjugation

An equal volume of a solution containing 24 mM of NHS and 12 mM of EDC was added to a suspension of GNPs at a concentration of 0.25 mM Au in 24 mM buffer MES at a pH of 6.0. The mixture was stirred at room temperature for 10 min, and the particles were centrifuged to remove remnants and resuspended in PBS.

The functionalized GNPs were incubated with a primary antibody against ENaC as previously described (Cerecedo et al., 2016). Briefly, approximately 3.5×10^{-3} μg/mL in a total volume of 100 μL of PBS were stirred together for 15 min at room temperature, 500 μL of BSA (0.3 mg/mL) was added to completely block any potential possible nonspecific binding sites on the surface of the GNPs-antiENaC conjugates. The complete volume was then maintained by stirring for 2.5 h at room temperature, then the conjugates were washed and separated by centrifugation and finally resuspended in PBS.

2.3.3. Characterization of functionalized GNPs and GNPs-antiENaC conjugates

The carboxy-terminated nanoparticles (GNPs-MPA) and the GNPs-antiENaC conjugates were characterized by FT-IR spectroscopy, the spectra were recorded using an ATR (Smart-iTX) accessory coupled with an FTIR spectrometer (Nicolet 912A0712 iS5). For UV-Vis measurements, each sample was analyzed in liquid form using a quartz cuvette in a Cary 5000 UV-Vis NIR spectrometer. Particle size determination and measurement of Zeta potential were carried out by dynamic light scattering (DLS, Zetasizer Nano-ZS90, Malvern Instruments). Electron micrographs were performed by transmission electron microscopy (JEOL, 2010 FE-TEM), and TEM grids were prepared by placing 7 μL of the diluted sample solution on carbon-coated films. Images were acquired at 120 kV.

2.4. Biosensing of ENaC in platelets by fluorescent assay

GNPs-antiENaC conjugates (absorbance ≈ 0.8 a.u. @ 540 nm) in a volume of 100 μL PBS were incubated for 1 h at room temperature with platelets samples of normotensive and hypertensive individuals (2.2 ×

10^6 platelets). After 1 h of incubation, a volume of secondary antibody labeled with Alexa Fluor 488 fluorophore ($\lambda_{excitation}$: 488 nm, $\lambda_{maxemission}$: 520 nm) was added and incubated for one additional hour at room temperature. After this time, the platelets were washed twice with PBS and separated by centrifugation at 500×*g* for 3 min. The fluorescence emission of the samples in PBS was measured in quartz cells with a Fluorolog model Jobin Yvon Horiba at an excitation wavelength of 490 nm.

3. Results

3.1. Functionalized gold nanoparticles features

The amount of MPA required to functionalize the GNPs was determined by keeping the GNPs concentration constant (~4.5×10^{10} particles/mL) while modulating the MPA concentration. To determine the concentration of MPA still suitable for the particle coating, we measured the size and Zeta potential of the GNPs after the addition of MPA. The Zeta potential values and the hydrodynamic diameters of unmodified and modified GNPs are shown in detail in Appendix A (Table A.2). Commercial GNPs (referred to as 'unmodified' in Table A.1) were originally stabilized by citrate ligands according to the manufacturer's instructions. Unmodified GNPs exhibited an average hydrodynamic diameter below 50 nm and a negative Zeta potential value of -36.7 ± 1.6 mV.

Results show that above 0.3 mM (MPA) correspond with larger changes in Zeta potential as well as a notable increase in hydrodynamic diameter, which can mainly be attributed to the fact that higher concentrations of AMP in dissolution implies decreases in pH values. Note that the most important factor that affects Zeta potential is the pH of the medium (Kulkarni and Sa, 2009).

GNPs were also characterized by UV−Vis absorption spectrometry. Unmodified particles possess a plasmonic band around 524 nm, and it is known that the shift and widening of the plasmonic band, in addition to the appearance of other bands at higher wavelengths, are indicative of an increase in particle size that is mainly attributed to agglomeration (Zuber et al., 2016) (Nietzold and Lisdat, 2012). In the UV-Vis spectra shown in Fig. 1, the colloidal stability of the GNPs with MPA concentrations equal to or higher than 1 mM was strongly affected by decreases in pH (Table A.3).

Conjugation was achieved by forming a peptide bond between the N-terminal amino group of antibodies and carboxylic groups exposed to the surface of GNPs after functionalization with MPA. Before addition of α-ENaC antibody, it was necessary to activate the carboxylic groups using EDC/NHS solution. Despite maintaining pH conditions using MES buffer at a pH of 6, the colloidal stability of GNPs was slightly lost after the addition of activation buffer, as evidenced by the spontaneous decrease of Zeta potential value (absolute value) from -37 mV to around -5 mV (Table 1) and the immediate color change from brilliant red to blue.

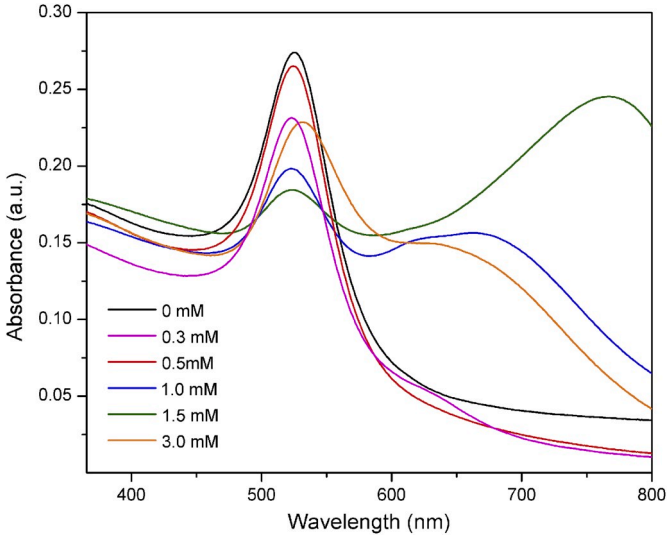

Fig. 1. UV-Vis absorption spectra of unmodified and different concentrations of AMP-modified GNPs. The particle concentration remained constant (around 4.5×10^{10} particles/mL).

To prevent nonspecific binding of GNPs to a variety of proteins present in the study system (human platelets), we used bovine serum albumin (BSA) to recover the non-blocked GNPs surface by the antibody through the formation of conjugates. The amount of BSA was varied from 0.0025 to 1 mg/mL while keeping the same particle concentration mentioned above and functionalized with MPA 0.04 mM. We observed that the progressive increase in the amount of albumin added contributed to restoring the surface charge of the NPs to Zeta potential values close to those measured before the activation buffer was added (Table 1). We selected a concentration of BSA of 0.3 mg/mL to accompany the GNPs-anti-ENaC conjugation procedure.

Using electron microscopy, we corroborated that the original size of the nanoparticles was approximately 30 nm, and we could also observe that after obtaining a total coating of the GNPs surface, the total diameter increased as much as we increased the concentration of albumin. Fig. 2a and b shows SEM and TEM images of BSA-coated GNPs using 1 and 0.3 mg/mL of albumin, respectively. We noted that 1 mg/mL of protein contributed to duplicate the diameter of the particles, while when we used only 0.3 mg/mL, the thickness of the protein layer was around 10 nm. Fig. 2c shows the spectra of albumin and GNPs-anti-ENaC conjugates using a concentration of 0.3 mg/mL of BSA for blocking the total nanoparticle surface. Both the α-ENaC antibody and BSA bound to the GNPs surface by EDC/NHS chemistry. We note that the band located at approximately 1650 cm^{-1} and corresponding to the amide bond (amide I, predominantly C = O *str*) (Myshakina et al., 2008) presented higher absorbance intensity in the conjugate spectrum as well as a slight frequency shift.

A schematic illustration of the MPA functionalization, the GNPs-BSA conjugation and the GNPs-GNP-antibody conjugates obtention in the presence of albumin are shown in Fig. 3 accompanied by their corresponding UV-Vis spectra. A progressive redshift in the plasmonic band was observed from the start to the end of the conjugation steps.

We next sought to determine the specificity of the antiENaC and GNPs conjugate to the ENaC present in platelets. We processed platelets as previously described and analyzed them using indirect immunofluorescence. Platelets were incubated with the GNPs-antiENaC conjugates followed by a secondary antibody labeled with the Alexa Fluor 488 fluorophore. We analyzed four different samples of 2×10^6 platelets each in presence of GNPs-GNP-antiENaC followed by the secondary antibody; as controls we included samples with 2×10^6 and 6×10^6 platelets incubated only with antiENaC without GNPs and GNPs-albumin and secondary antibody. As shown in Fig. 4, the fluorescence

Table 1
Measurements carried out in water in a Zetasizer Nano-ZS90 equipment, the measurement of each sample was repeated three times.

GNPs-AMP + BSA [mg/mL]	Size (nm) ± SD	PdI	Zeta pot (mV) ± SD
0.0025	213 ± 5	>0.6	-5.7 ± 1.03
0.003	238 ± 12	>0.6	-13.7 ± 1.8
0.005	286 ± 9	>0.6	-18.8 ± 5.4
0.01	261 ± 3	>0.6	-27.8 ± 7.3
0.02	241 ± 2	>0.6	-23.4 ± 4.2
0.03	237 ± 7	0.4	-24.2 ± 6.1
0.04	235 ± 4	0.6	-33.7 ± 8
0.1	202 ± 7	0.4	-27.3 ± 1.3
0.2	178 ± 8	0.6	-29.7 ± 1.8
0.3	162 ± 2	0.6	-31.3 ± 3.4
0.6	165 ± 7	0.5	-37.2 ± 6.7
1.0	169 ± 17	0.5	-31.4 ± 3.6

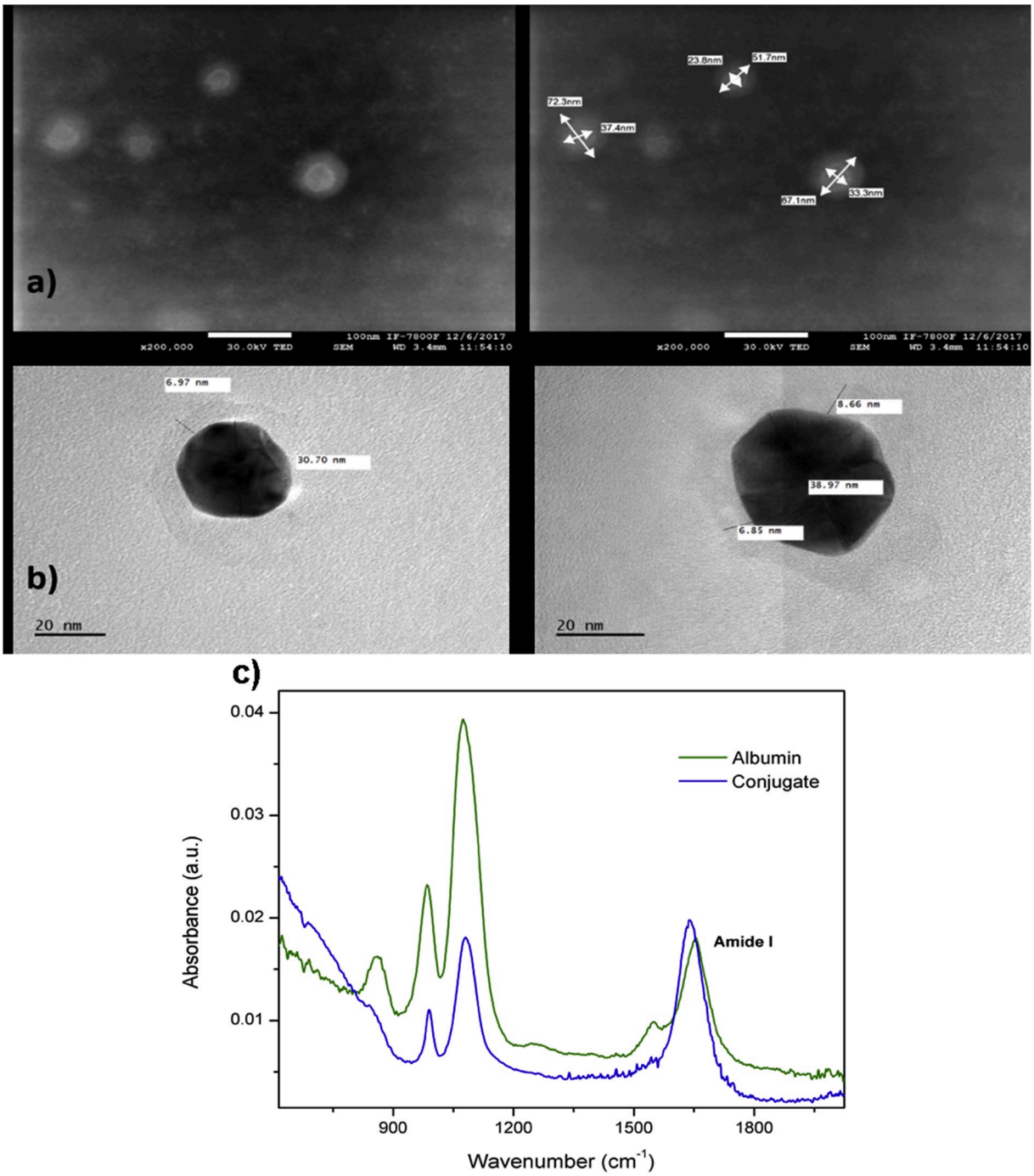

Fig. 2. Electron micrographs a) GNPs-BSA using a concentration of 1 mg/mL of albumin (SEM) and b) GNPs-BSA using a concentration of 0.3 mg/mL of albumin (TEM), c) FTIR-ATR absorbance spectra of albumin and GNPs-antiENaC conjugates.

intensity is higher in platelets treated with the conjugates than in control samples. Additionally, compared with samples treated only with primary antibody the presence of GNPs increased the fluorescence intensity of the platelet samples.

Taken together, these results strongly suggest a specific increase in the fluorescence intensity values due to the direct interaction between the conjugates and the ENaC expressed on the platelets' plasma membrane.

3.2. Potential use of GNPs-antiENaC as a diagnostic tool for hypertension

According to the results described in the previous section, the GNPs-antiENaC conjugates generated in the present study bind specifically to ENaC in platelets. ENaC is overexpressed in platelets from hypertensive patients (Cerecedo et al., 2016). To evaluate if the fluorescence emission changed based on the type of samples, we processed platelets from hypertensive or normotensive individuals. First, we compared fluorescence spectra at different platelet concentrations from these two groups who maintained the same concentration of GNPs-anti-ENaC conjugates as well as secondary antibodies. We expected that both kinds of samples would increase the fluorescence values as the platelet concentration increased. This linear behavior was observed until 2×10^6 platelets remained and, at this point we observed a clear difference between normotensive individuals and hypertensive patients (Fig. 5a). In

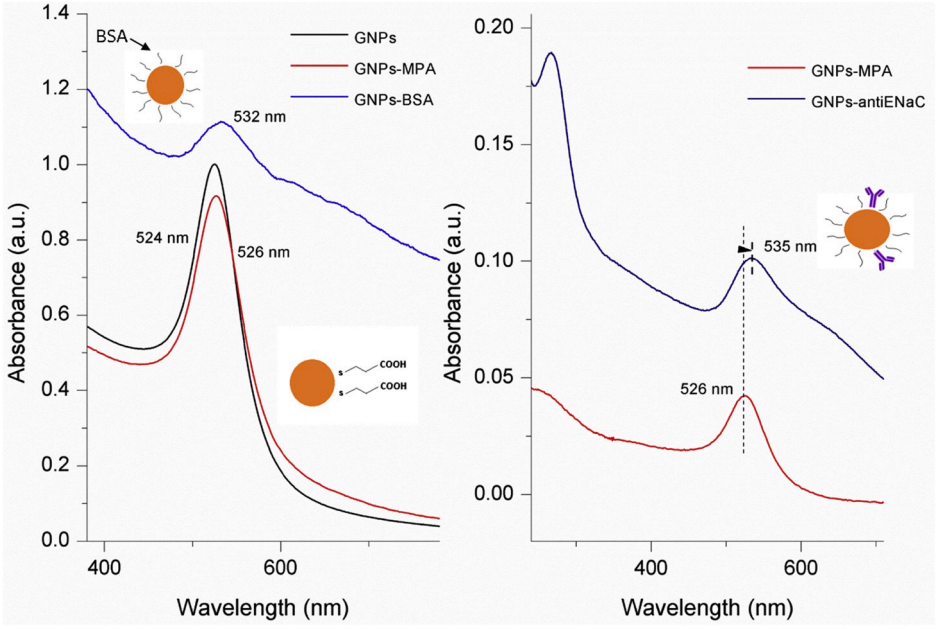

Fig. 3. UV-Vis spectra of GNPs, GNPs functionalized with MPA, GNPs covalently bound to BSA and GNPs-antiENaC conjugates.

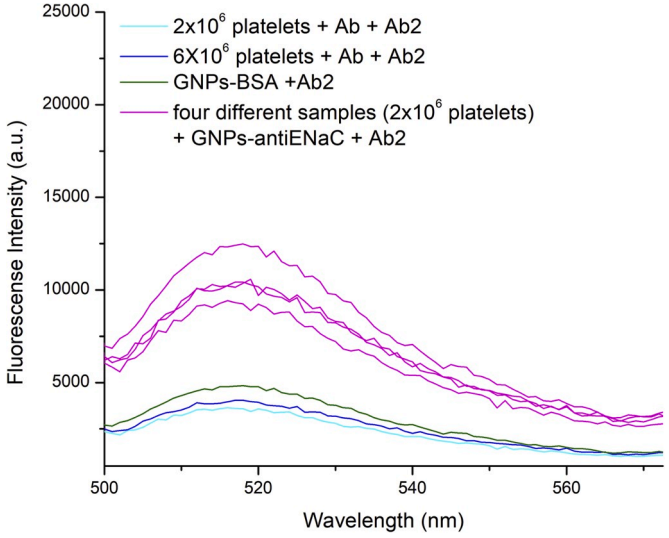

Fig. 4. a) Fluorescence spectra of platelets in low (2×10^6) and high (6×10^6) amounts of platelets incubated with Ab:α-ENaC antibody or GNPs-antiENaC: conjugates, followed by Ab2:secondary antibody conjugated to Alexa Fluor. GNPs-BSA were incubated with Ab2 and measured as a control.

contrast, the highest platelet concentrations reduced notably in fluorescence emissions. The results are representative of five different samples; we also observed high dispersion fluorescence intensity values, mainly in platelets from hypertensive patients.

A concentration of 2×10^6 platelets allowed us to see greater differences between the fluorescence emission values in hypertensive versus normotensive samples (Fig. 5b); high dispersion values were characteristic of hypertensive samples. Although mean fluorescence intensity values were not significantly different, the data as a whole showed a clear tendency to separate into "low" and "high" fluorescence intensity clusters for normotensive and hypertensive samples, respectively (Fig. 5c). The fluorescence intensity values were associated with the amount of ENaC on the platelets' plasma membranes.

4. Discussion

In the present study, we functionalized GNPs by binding with the epithelial sodium antibody (antiENaC), our two-step procedure preserved colloidal stability and antibody-antigen binding capacity. First, the particles were functionalized using MPA, which is a bifunctional molecule that binds strongly to AuNPs through the thiol group (Pensa et al., 2012). This ligand provides a negative charge to the surface of the GNPs (Nilam et al., 2019) and according to the Zeta potential and DLS measurements allowed to preserve the colloidal stability as much as in the case of unmodified GNPs. When we used MPA concentrations between 0.07 and 0.04 mM, the hydrodynamic diameters decreased, and the Zeta potential improved. Zeta potential is the electric potential in the interfacial double layer of a dispersed particle versus a point in the continuous phase away from the interface (Lu and Gao, 2010). This value is often used as a key indicator of the stability of colloidal dispersions, where values that are more positive than +30 mV and more negative than −30 mV indicate good stability against coalescence (Kadu et al., 2011). At higher concentrations of MPA, loss of colloidal stability was immediately visible, mainly since the excess in solution of this compound can easily modify the pH of the nanoparticle solution.

The second step consisted of the activation of carboxylic groups followed by antiENaC and BSA addition. We decided to use BSA because it is considered to be a universal blocking reagent and helps to prevent the non-specific binding of the conjugates to any platelet proteins different to ENaC in many applications. It also contributes to restore the negative surface charge on the surface of the nanoparticles and the colloidal stability in their conjugated form. The conjugation process was characterized by spectroscopic and microscopic techniques, and the GNPs surface plasmon resonance (SPR) was monitored for UV-Vis spectroscopy (Fig. 3). The original wavelength of maximum absorbance in the unmodified particles was centered at 524 nm. After functionalization with MPA, the SPR suffered a slight red shift to 526 nm. When the particles were covered with BSA, and for BSA/antiENaC, the red shift resulted in 532 and 535 nm, respectively. This plasmonic shift was the product of a change in the local refractive index as a result of the protein/antibody adlayer (Tripathi and Driskell, 2018). Using FTIR-ATR spectroscopy, we could observe that the amide I band presented higher absorbance intensity in the conjugate spectrum as well as a slight frequency shift in comparison with the BSA spectrum. This might be

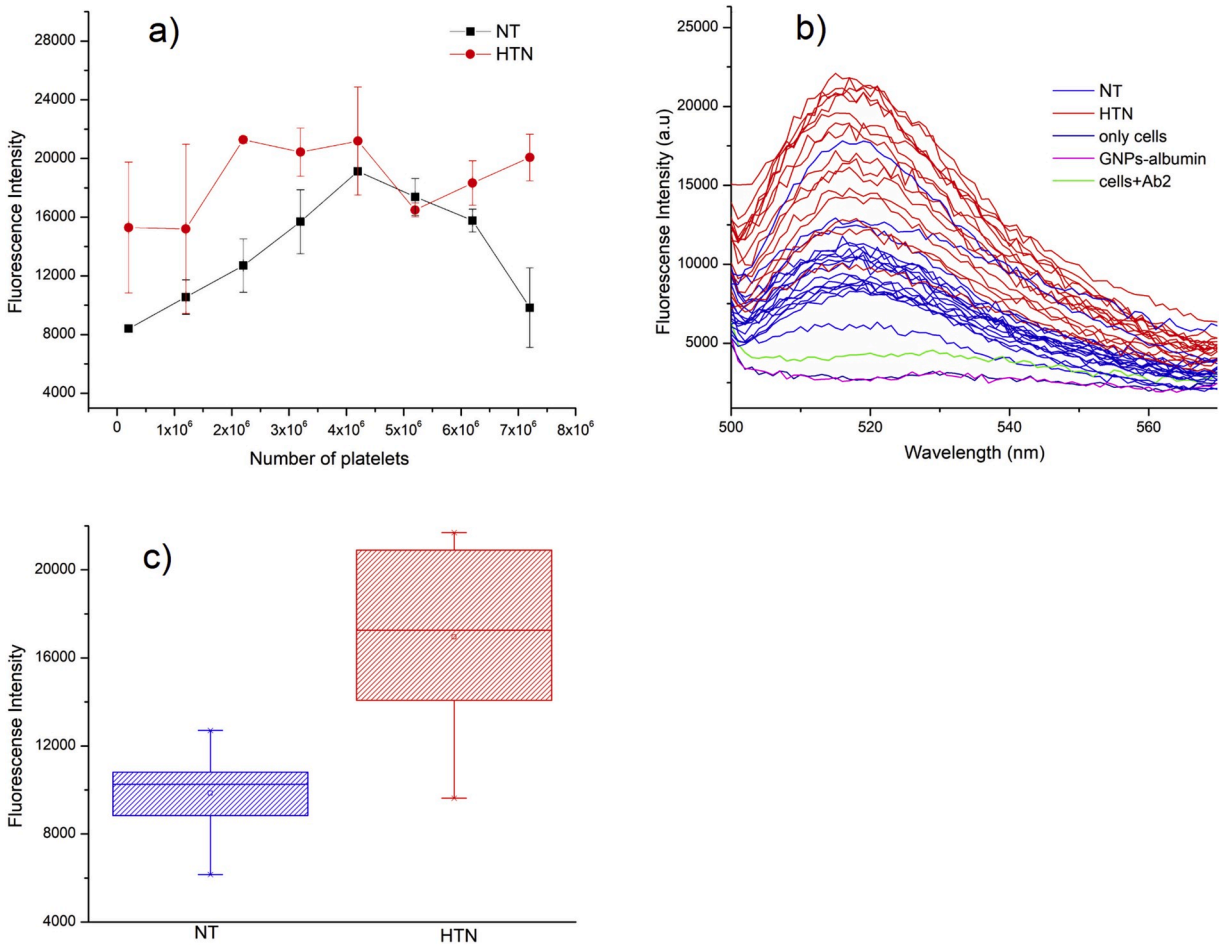

Fig. 5. a) Fluorescence intensity values *versus* the number of platelets used in the fluorescent assay; b) Fluorescence emission spectra of platelets samples of healthy and hypertensive individuals λ_{exc} of 488 nm (495–570 nm), c) Mean fluorescence emission intensity of platelets samples (HTN: NH, number of samples 19:16).

interpreted as evidence that GNPs-antiENaC conjugates were forming by covalent binding. However, these methods are not sufficient to verify that the antibody-antigen binding capacity is preserved despite antibody immobilization onto the GNPs surface. In order to prove the permanence of the antibody-GNPs binding after washes and centrifugation cycles implied within the conjugation procedure, and more importantly, the antigen-antibody binding capacity of antiENaC in its conjugated form, we proposed a fluorescent immunoassay to be directly carried out in platelets as a semi-quantitative strategy to describe the effect of nanoparticles on the fluorescence emission of a second antibody used. This method also found interesting differences when we compared the fluorescent emissions obtained in normotensive versus hypertensive platelets. The fluorescent intensity spectra shown in Fig. 4 were an indication of fluorescent enhancement as a consequence of the presence of GNPs. We previously compared the fluorescent intensity depending on the number of platelets using a fluorescent detection assay and corroborated that fluorescence intensity increased as much as we incremented the number of platelets used (data no showed). As shown in Fig. 4, despite that we used the same and higher number of cells, samples treated with GNPs-anti-ENaC conjugates showed a larger intensity regime regarding to platelets treated only with α-ENaC antibody. It is known that the fluorescence intensity of a given fluorophore can be altered in different ways when it is placed near an entity possessing an electromagnetic field (e.g., in the case of plasmons in metal nanoparticles) (Kang et al., 2011). When the metal surface is close, the luminous efficiency of the fluorescent molecule can be enhanced (Chen et al., 2013) or quenched depending on the distance between the metal surface and the fluorophore (Kang et al., 2011) (Chen et al., 2013; Kandela and Albrecht, 2007). Our evidence suggests that the distance provided by indirect conjugation (e.g., the use of MPA as a short ligand) is sufficient to avoid the quenching effect reported by several authors in cases of direct conjugation (very small distances) of the fluorophore onto metallic nanoparticle surfaces and instead moderately enhances fluorescence emission.

The amount of nanoparticles, size, shape, wavelength excitation and types of fluorophore are other important features that can affect fluorescence emission (Qin et al., 2018). We selected Alexa Fluor secondary antibody because we have previously used for ENaC detection by immunofluorescence assays using the same antiENaC that we conjugated with the GNPs (Cerecedo et al., 2016). This fluorescent dye absorbs light and emits fluorescence at wavelengths within the plasmonic band of GNPs. We performed an analysis of the fluorescence response at different platelets concentration (Fig. 5a) the number of cells used was an important factor to potentiate the difference between the fluorescence intensity obtained with the HTN platelets assays and those with NT, maintaining the same concentration of conjugates and secondary antibodies, the notable higher fluorescent intensity values exhibited in the HTN sample compared to the NT sample was mainly reinforced when we used a concentration of 2×10^6 platelets.

Gradual decreases in fluorescence emissions after exceeding a certain number of cells is probably attributed to the reduction of target sites of each cell as the number of cells increases. This tendency was not as clear in NT platelets as in HTN platelets, where probably the distribution of binding sites and distances between flourophore GNPs arrays are affected by irregularities of cell membrane and cytoskeleton derived from a pre-activated state (Cerecedo et al., 2016). We observed diverse

fluorescent responses between the platelet samples analyzed, and they are suggestive of biological variability. Finally, in our future work we will analyze 100 individuals and use the ROC statistical method to identify a threshold and to better understand the sensitivity and specificity of our proposed assay.

5. Conclusions

In this work, we successfully functionalized GNPs into covalently bonded GNPs-antiENaC conjugates. Analysis by Zeta potential, dynamic light scattering, electron microscopy, and other spectroscopic methods confirmed the association between the GNPs and the α-ENaC antibody. The specificity of the conjugates was evidenced by indirect immunofluorescence after incubation with human platelets. Our results indicate that fluorescence intensity is associated with the presence of ENaC on the platelet's plasma membrane. This enables discriminating between hypertensive and normotensive individuals, which represents a useful diagnostic tool for HTN.

Declaration of competing interest

The authors declare that they have no known competing financial interests or personal relationships that could have appeared to influence the work reported in this paper.

CRediT authorship contribution statement

Diana L. García-Rubio: Conceptualization, Investigation, Methodology, Validation, Writing - original draft. **M.B. de la Mora:** Conceptualization, Investigation, Methodology, Writing - original draft. **Doris Cerecedo:** Funding acquisition, Conceptualization, Investigation, Methodology, Writing - original draft. **José M. Saniger Blesa:** Conceptualization, Writing - review & editing, Supervision. **M. Villagrán-Muniz:** Funding acquisition, Supervision, Writing - review & editing.

Acknowledgements

We want to acknowledge the financial support received from the project: Proyecto No. 9230c19, de la Secretaría de Educación, Ciencia, Tecnología e Innovación de la CDMX, PAPIIT project IG100418 from DGAPA UNAM and projects A1-S-23112 and A1-S-22695 from Ciencia Básica CONACyT.. Also, Dr. Mayo Villagran would like to thank the support of DGAPA-UNAM for the support for his sabbatical year. Doris Cerecedo want to thank to project SIP 20180778. Diana Garcia thank to CONACyT Becas Nacionales for the scholarship given (number 449505). Authors want to thank Victor Duarte Alaniz from Department of Physical Chemistry from Institute of Chemistry UNAM for the artwork present in this manuscript.

All authors want to thank Selene R. Islas Sánchez from LUCE-UNAM and Viridiana Maturano from LUNA-UNAM for their technical support in the FTIR-ATR and spectrofluorometer characterization and Zeta potential measurements, respectively. We want to thank as well all the facilities that the laboratories LUCE-UNAM and LUNA-UNAM give for the development of this research. The authors would also like to thank to Roberto Hernández Reyes from IF-UNAM for conducting the TEM measurements, Dr. Samuel Tehuacanero Cuapa from SEM measurements and Diego Quiterio Vargas for his technical support for TEM and SEM samples preparation.

Appendix A. Supplementary data

Supplementary data to this article can be found online at https://doi.org/10.1016/j.bios.2020.112151.

References

Acuna, G., Möller, F., Holzmeister, P., Beater, S., Lalkens, B., Tinnefeld, P., 2012. Fluorescence enhancement at docking sites of DNA-directed self-assembled nanoantennas. Science 338 (6106), 506–510.
Bartczak, D., Kanaras, A.G., 2011. Preparation of peptide-functionalized gold nanoparticles using one pot EDC/sulfo-NHS coupling. Langmuir 27 (16), 10119–10123.
Bhalla, V., Hallows, K.R., 2008. Mechanisms of ENaC regulation and clinical implications. J. Am. Soc. Nephrol. 19 (10), 1845–1854.
Borisov, S.M., Wolfbeis, O.S., 2008. Optical biosensors. Chem. Rev. 108 (2), 423–461.
Cerecedo, D., Martínez-Vieyra, I., Sosa-Peinado, A., Cornejo-Garrido, J., Ordaz-Pichardo, C., Benítez-Cardoza, C., 2016. Alterations in plasma membrane promote overexpression and increase of sodium influx through epithelial sodium channel in hypertensive platelets. Biochim. Biophys. Acta Biomembr. 1858 (8), 1891–1903.
Chen, Y.-C., Gao, C.-Y., Chen, K.-L., Meen, T.-H., Huang, C.-J., 2013. Enhancement and quenching of fluorescence by silver nanoparticles in organic light-emitting diodes. J. Nanomater. 16, 2013.
Devi, R.V., Doble, M., Verma, R.S., 2015. Nanomaterials for early detection of cancer biomarker with special emphasis on gold nanoparticles in immunoassays/sensors. Biosens. Bioelectron. 68, 688–698.
Doria, G., Conde, J., Veigas, B., Giestas, L., Almeida, C., Assunção, M., Rosa, J., Baptista, P.V., 2012. Noble metal nanoparticles for biosensing applications. Sensors 12 (2), 1657–1687.
Enuka, Y., Hanukoglu, I., Edelheit, O., Vaknine, H., Hanukoglu, A., 2012. Epithelial sodium channels (ENaC) are uniformly distributed on motile cilia in the oviduct and the respiratory airways. Histochem. Cell Biol. 137 (3), 339–353.
Hanukoglu, I., Hanukoglu, A., 2016. Epithelial sodium channel (ENaC) family: phylogeny, structure–function, tissue distribution, and associated inherited diseases. Gene 579 (2), 95–132.
Iosin, M., Toderas, F., Baldeck, P., Astilean, S., 2009. Study of protein–gold nanoparticle conjugates by fluorescence and surface-enhanced Raman scattering. J. Mol. Struct. 924, 196–200.
Kadu, P.J., Kushare, S.S., Thacker, D.D., Gattani, S.G., 2011. Enhancement of oral bioavailability of atorvastatin calcium by self-emulsifying drug delivery systems (SEDDS). Pharmaceut. Dev. Technol. 16 (1), 65–74.
Kandela, I.K., Albrecht, R.M., 2007. Fluorescence quenching by colloidal heavy metals nanoparticles: implications for correlative fluorescence and electron microscopy studies. Scanning: J. Scanning Microsc. 29 (4), 152–161.
Kang, K.A., Wang, J., Jasinski, J.B., Achilefu, S., 2011. Fluorescence manipulation by gold nanoparticles: from complete quenching to extensive enhancement. J. Nanobiotechnol. 9 (1), 16.
Kulkarni, R.V., Sa, B., 2009. Polyacrylamide-grafted-alginate-based pH-sensitive hydrogel beads for delivery of ketoprofen to the intestine: in vitro and in vivo evaluation. J. Biomater. Sci. Polym. Ed. 20 (2), 235–251.
Larguinho, M., Baptista, P.V., 2012. Gold and silver nanoparticles for clinical diagnostics—from genomics to proteomics. J. Proteom. 75 (10), 2811–2823.
Lazarides, A., Kelly, K.L., Jensen, T., Schatz, G.C., 2000. Optical properties of metal nanoparticles and nanoparticle aggregates important in biosensors. J. Mol. Struct.: THEOCHEM 529 (1-3), 59–63.
Lu, G.W., Gao, P., 2010. Emulsions and Microemulsions for Topical and Transdermal Drug Delivery. Handbook of Non-invasive Drug Delivery Systems. Elsevier, pp. 59–94.
Martínez-Vieyra, I., García-Rubio, D., De la Mora-Mojica, B., Durán-Álvarez, J.C., Rodriguez-Varela, M., Méndez-Méndez, J.V., Cerecedo, D., 2019. Alterations to plasma membrane lipid contents affect the biophysical properties of erythrocytes from individuals with hypertension. Biochim. Biophys. Acta Biomembr. 1861 (10), 1–9, 182996. In press.
Mascini, M., Tombelli, S., 2008. Biosensors for biomarkers in medical diagnostics. Biomarkers 13 (7-8), 637–657.
Myshakina, N.S., Ahmed, Z., Asher, S.A., 2008. Dependence of amide vibrations on hydrogen bonding. J. Phys. Chem. B 112 (38), 11873–11877.
Nakamura, T., Hayashi, S., 2005. Enhancement of dye fluorescence by gold nanoparticles: analysis of particle size dependence. Jpn. J. Appl. Phys. 44 (9R), 6833.
Nietzold, C., Lisdat, F., 2012. Fast protein detection using absorption properties of gold nanoparticles. Analyst 137 (12), 2821–2826.
Nilam, M., Ahmed, M., Alnajjar, M.A., Hennig, A., 2019. Characterization of mixed-ligand shells on gold nanoparticles by transition metal and supramolecular surface probes. Analyst 144 (2), 579–586.
Organization, W.H., 2019. Hypertension. World Health Organization.
Pensa, E., Cortes, E., Corthey, G., Carro, P., Vericat, C., Fonticelli, M.H., Benitez, G., Rubert, A.A., Salvarezza, R.C., 2012. The chemistry of the sulfur–gold interface: in search of a unified model. Accounts Chem. Res. 45 (8), 1183–1192.
Qian, X.-M., Nie, S.M., 2008. Single-molecule and single-nanoparticle SERS: from fundamental mechanisms to biomedical applications. Chem. Soc. Rev. 37 (5), 912–920.
Qin, H., Ma, D., Du, J., 2018. Distance dependent fluorescence quenching and enhancement of gold nanoclusters by gold nanoparticles. Spectrochim. Acta Mol. Biomol. Spectrosc. 189, 161–166.
Quarta, A., Curcio, A., Kakwere, H., Pellegrino, T., 2012. Polymer coated inorganic nanoparticles: tailoring the nanocrystal surface for designing nanoprobes with biological implications. Nanoscale 4 (11), 3319–3334.
Reus-Chavarría, E., Martínez-Vieyra, I., Salinas-Nolasco, C., Chávez-Piña, A.E., Méndez-Méndez, J.V., López-Villegas, E.O., Sosa-Peinado, A., Cerecedo, D., 2019. Enhanced

expression of the Epithelial Sodium Channel in neutrophils from hypertensive patients. Biochim. Biophys. Acta Biomembr. 1861 (2), 387–402.
Schneider, G., Decher, G., Nerambourg, N., Praho, R., Werts, M.H., Blanchard-Desce, M., 2006. Distance-dependent fluorescence quenching on gold nanoparticles ensheathed with layer-by-layer assembled polyelectrolytes. Nano Lett. 6 (3), 530–536.
Tripathi, K., Driskell, J.D., 2018. Quantifying bound and active antibodies conjugated to gold nanoparticles: a comprehensive and robust approach to evaluate immobilization chemistry. ACS Omega 3 (7), 8253–8259.
Zuber, A., Purdey, M., Schartner, E., Forbes, C., van der Hoek, B., Giles, D., Abell, A., Monro, T., Ebendorff-Heidepriem, H., 2016. Detection of gold nanoparticles with different sizes using absorption and fluorescence based method. Sensor. Actuator. B Chem. 227, 117–127.